

Rethinking Barely-Supervised Segmentation from an Unsupervised Domain Adaptation Perspective

Zhiqiang Shen^{1,2}, Peng Cao^{1,2*}, Junming Su^{1,2}, Jinzhu Yang^{1,2}, and Osmar R. Zaiane³

¹ School of Computer Science and Engineering, Northeastern University, Shenyang, China

² Key Laboratory of Intelligent Computing in Medical Image, Ministry of Education, Shenyang, China
xszqyy@gmail.com

³ Alberta Machine Intelligence Institute, University of Alberta, Edmonton, Alberta, Canada

Abstract. This paper investigates an extremely challenging problem, barely-supervised medical image segmentation (BSS), where the training dataset comprises limited labeled data with only single-slice annotations and numerous unlabeled images. Currently, state-of-the-art (SOTA) BSS methods utilize a registration-based paradigm, depending on image registration to propagate single-slice annotations into volumetric pseudo labels for constructing a complete labeled set. However, this paradigm has a critical limitation: the pseudo labels generated by image registration are unreliable and noisy. Motivated by this, we propose a new perspective: training a model using only single-annotated slices as the labeled set without relying on image registration. To this end, we formulate BSS as an unsupervised domain adaptation (UDA) problem. Specifically, we first design a novel noise-free labeled data construction algorithm (NFC) for slice-to-volume labeled data synthesis, which may result in a side effect: domain shifts between the synthesized images and the original images. Then, a frequency and spatial mix-up strategy (FSX) is further introduced to mitigate the domain shifts for UDA. Extensive experiments demonstrate that our method provides a promising alternative for BSS. Remarkably, the proposed method with **only one** labeled slice achieves an 80.77% dice score on left atrial segmentation, outperforming the SOTA by 61.28%. The code will be released upon the publication of this paper.

Keywords: Barely-Supervised Learning · Medical Image Segmentation · Unsupervised Domain Adaptation.

* Corresponding author

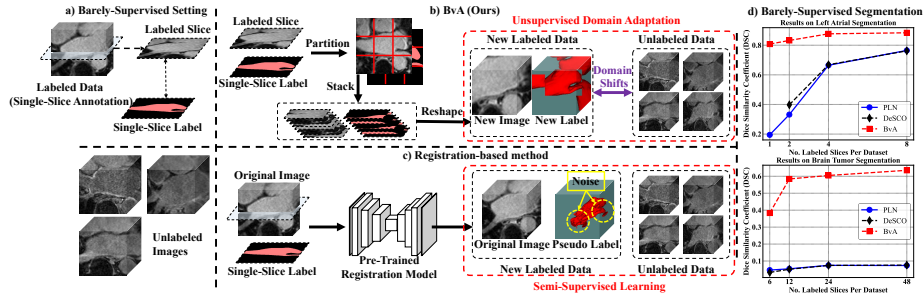


Fig. 1. Illustration of a) barely-supervised setting, b) our BvA, c) the registration-based paradigm, and d) barely-supervised segmentation results. Note that DeSCO requires two orthogonal labeled slices per image; therefore, it is unavailable for the situation where the training set contains only one labeled slice.

1 Introduction

Medical image segmentation for delineating organs and tumors is essential for clinical applications. Considerable advances have been made based on supervised learning, relying on large-scale **fully and completely** annotated datasets that the entire dataset is fully annotated and each sample has a complete label. However, annotating medical images at the pixel level is laborious and requires expert knowledge, resulting in a significant annotation burden. Semi-supervised learning (SSL) [16,10,14] and weakly-supervised learning (WSL) [20,19] are two prevailing paradigms for alleviating the annotation burden on medical image segmentation. Nevertheless, there are still hundreds and thousands of slices that need to be labeled at the pixel level.

Barely-supervised learning (BSL) based medical volumetric image segmentation, abbreviated as BSS, has the potential to further reduce annotation costs [3], with the setting [Fig. 1(a)] only requiring a **partially and incompletely** annotated dataset comprising a barely-annotated labeled set with single-slice annotations and a large number of unlabeled images. *The key challenge in BSS is how to generate volumetric labels from single-slice annotations for constructing a complete labeled set.* State-of-the-art (SOTA) BSS methods [7,4] rely on a registration-based paradigm. As illustrated in Fig. 1(c), this paradigm first generates pseudo labels for the other slices in a volume from the single-annotated slice by image registration, thereby transforming the barely-annotated labeled set into a completely annotated labeled set. The goal of the registration-based methods is to transform BSS into a semi-supervised learning problem. However, this paradigm has a critical limitation: the pseudo labels generated by image registration are unreliable and noisy, degrading the training process. We conducted a pilot experiment to investigate the effect of the limitation on BSS. As shown in Fig. 1(d), PLN [7] and DeSCO [4] obtain inferior performance on left atrial segmentation, especially in scenarios with only one or two annotated slices

in the training set. The results become even more unsatisfactory in the more challenging brain tumor segmentation task with heterogeneous tumors.

We propose a novel BSS framework, **B**arely-supervised learning **via** unsupervised domain **A**daptation (BvA) [Fig. 1(b)]. As depicted in Fig. 1(d), BvA consistently outperforms the registration-based methods by a large margin that exceeds 60% in terms of the Dice similarity coefficient (DSC) in the situation where the entire training set contains **only one** labeled slice. Considering the limitation of the registration-based paradigm, we explore a new perspective: *Is it feasible to train a model using only barely-annotated slices as the labeled set, without relying on image registration?* To this end, BvA formulates BSS as an unsupervised domain adaptation (UDA) problem (source domain: the synthesized images, target domain: the original images). Specifically, we first introduce a noise-free labeled data construction algorithm (NFC) for slice-to-volume labeled data synthesis from single-annotated slices by deconstructing a slice into patches and reconstructing a volumetric image from the patches. The idea of NFC lies in that the inter-patch similarity in a slice is akin to the inter-slice continuity of a volume. However, NFC may result in a negative effect: the synthesized images differ from the original images in terms of image spacing and anatomical structures, which can be considered as domain shifts in style and content, respectively. To this end, we assume that a well-generalized model should behave smoothly across both source and target domains under small perturbations. We further design a frequency and spatial mix-up strategy (FSX), which performs mix-up [18] in the frequency [15,13] and spatial [17] domains to mitigate the style and content shifts respectively for UDA. Extensive experiments show that BvA significantly improves the state-of-the-art results on the left atrial and brain tumor segmentation benchmarks under both **barely-supervised segmentation** and **semi-supervised segmentation** settings. For example, BvA achieves 87.71% in terms of DSC on the LA dataset with 5% barely-labeled data (only 4 labeled slices in the training set) and a DSC of 58.42% on the BraTS dataset with 5% barely-labeled data (only 12 labeled slices), outperforming PLN [7] by 21.25% and 53.01%, respectively.

Our contributions mainly include:

- It is the first work to formulate BSS as a UDA problem by constructing a complete volumetric labeled set from single-annotated slices without requiring image registration.
- Based on the smoothness assumption, we further propose FSX for UDA to mitigate the introduced domain shifts.
- We conduct extensive experiments on two public medical image segmentation datasets including organ and tumor segmentation. Comprehensive results demonstrate the advantage of BvA over state-of-the-art for the BSS task.

2 Method

We first define barely-supervised medical image segmentation (BSS). The training set $\mathcal{D} = \{\mathcal{D}^L, \mathcal{D}^U\}$ includes a barely labeled set $\mathcal{D}^L = \{(X_i^l, y_{i(k)}^l)_{i=1}^{N_L}\}$ and an

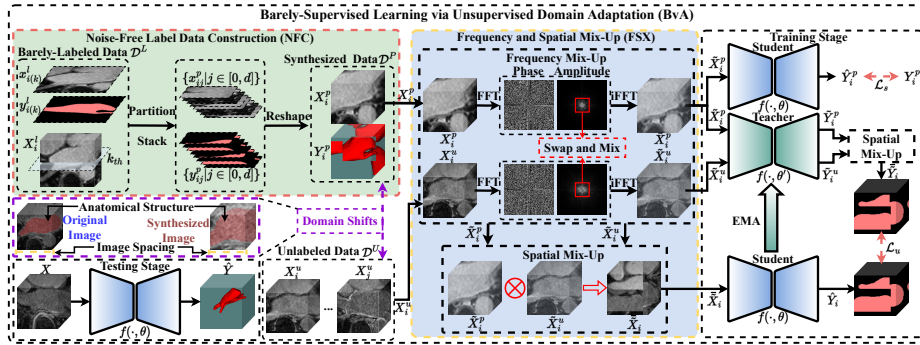


Fig. 2. The schematic diagram of the proposed Barely-supervised learning via unsupervised domain Adaptation (BvA). BvA consists of 1) a noise-free labeled data construction algorithm (NFC) for generating volumetric labeled data, and 2) a frequency and spatial mix-up strategy (FSX) for alleviating domain shifts between the synthesized images and the original images. Note that BvA only requires a single segmentation model in the testing stage.

unlabeled set $\mathcal{D}^U = \{(X_i^u)_{i=1}^{N^U}\}$, where X_i^l/X_i^u denotes the i_{th} labeled/unlabeled image, $y_{i(k)}^l$ is the single-slice annotation of the k_{th} slice $x_{i(k)}^l$ for the i_{th} labeled image X_i^l , and N^L and N^U ($N^U \gg N^L$) are the numbers of labeled and unlabeled samples. BSS aims to learn a model $f(\cdot; \theta)$ from the partially and incompletely annotated training data \mathcal{D} , to perform well on unseen test sets.

2.1 Barely-Supervised Learning via Unsupervised Domain Adaptation (BvA)

Considering the limitation of the registration-based paradigm, we investigate a new perspective for BSS: training a segmentation model using only single-annotated slices as the labeled set. Conceptually, we formulate BSS as a UDA problem. As illustrated in Fig. 2, to realize this conception, BvA includes two components: 1) a noise-free labeled data construction algorithm (NFC) for constructing a complete volumetric labeled set from the barely-annotated data and 2) a frequency and spatial mix-up strategy (FSX) to mitigate domain shifts between the synthesized images and the original images for UDA.

Noise-Free Labeled Data Construction (NFC) The key challenge in BSS is how to generate volumetric labels from single-slice annotations for constructing a complete labeled set. Inspired by the observation that the inter-patch similarity in a slice resembles the inter-slice continuity of a volume, we develop NFC to synthesize volumetric image-label pairs using only single-annotated slices. Formally, NFC involves the following steps: **1) Partitioning** a single-annotated slice $x_{i(k)}^l$ (and its corresponding annotation $y_{i(k)}^l$) into patches using a slide win-

dow strategy⁴: $\{x_{ij}^p | j \in [1, d]\} = \text{Partition}(x_{i(k)}^l, r, s)$, **2) stacking** the patches $\{x_{ij}^p | j \in [1, d]\}$ into a small volume: $Z_i^p = \text{Stack}(\{x_{ij}^p | j \in [1, d]\})$, and **3) reshaping** the small volume Z_i^p to the same size as the original volumetric image X_i^l : $X_i^p = \text{Resize}(Z_i^p)$ where $\text{Partition}(\cdot)$, $\text{Stack}(\cdot)$, and $\text{Resize}(\cdot)$ denote the partitioning, stacking, and reshaping functions, respectively. d represents the depth of a synthesized image, depending on two hyperparameters: the window size r and the stride s . We determine r and s according to the following criteria: choosing a larger r to guarantee similarity between patches and the corresponding slices, while setting a smaller s to ensure that the partitioned patches are sufficient for constructing images with the number of slices similar to the original images.

Frequency and Spatial Mix-up (FSX) Based on the smoothness assumption across both the source and target domains, FSX conducts frequency mix-up and style mix-up to bridge the style and content gaps, respectively. We enforce the model’s predictions to remain invariant under frequency mix-up, which perturbs the style while preserving the content information of images [15,13]. Moreover, the model’s prediction under spatial mix-up that perturbs the content by mixing image regions is regularized to be consistent with the prediction for an image under the same spatial mix-up. In other words, we encourage the model to yield equivariant predictions under spatial mix-up.

Frequency Mix-Up (FX) performs mix-up between the amplitude components of an original image X_i^u and a synthesized image X_i^p :

$$\mathcal{A}(X) = (1 - \alpha)(1 - \Omega)\mathcal{A}(X_i^u) + \alpha\Omega\mathcal{A}(X_i^p) \quad (1)$$

where $\mathcal{A}(\cdot)$ denotes the mixed amplitude component, α controls the mix-up strength, and Ω is a center rectangle binary mask used to determine the mix-up range of amplitude spectrum [15,13]. Then, the style-perturbed images are generated by inverse Fourier transformation on the mixed amplitude component and the original phase components.

Spatial Mix-Up (SX) involves the CutMix [17] operation between the original images and the synthesized images:

$$\bar{X}_i = X_i^u \times M + X_i^p \times (1 - M) \quad (2)$$

where M is a random binary mask for image region mixing. Correspondingly, the CutMix operation should be applied to the segmentation maps: $\bar{Y}_i = \bar{Y}_i^u \times M + \bar{Y}_i^p \times (1 - M)$, where \bar{Y}_i^u and \bar{Y}_i^p are the pseudo labels of X_i^u and X_i^p .

Training Objective The training loss of BvA is defined as: $\mathcal{L} = \mathcal{L}_s + \mathcal{L}_u$, where \mathcal{L}_s and \mathcal{L}_u represent the supervised and unsupervised losses, respectively. Concretely, \mathcal{L}_s includes two terms for the barely-annotated data and the synthesized complete labeled set:

$$\mathcal{L}_s = \mathcal{L}_{seg} \left(f \left(x_{i(k)}^l; \theta \right), y_{i(k)}^l \right) + \mathcal{L}_{seg} \left(f \left(X_i^p; \theta \right), Y_i^p \right) \quad (3)$$

⁴ We omit the equations of $y_{i(k)}^l$ for brevity in explanation, as the procedure applied to both $x_{i(k)}^l$ and $y_{i(k)}^l$ is consistent.

where $f(\cdot; \theta)$ denotes the segmentation backbone and \mathcal{L}_{seg} can be any segmentation loss. Moreover, \mathcal{L}_u involves consistency regularization between the predicted segmentation maps for the original and perturbed images:

$$\mathcal{L}_u = \mathcal{L}_{seg}(f(X_i; \theta), \bar{Y}_i) \quad (4)$$

where X_i denotes the perturbed image and \bar{Y}_i refers to the mixed pseudo label.

3 Experiments and Results

3.1 Datasets

We evaluate the proposed BvA on the Left Atrial Segmentation 2018 (LA) [12] and Brain Tumor Segmentation 2020 (BraTS) [8,1,2] datasets. LA contains 100 gadolinium-enhanced MRI scans. Following [16], we split LA into 80 samples for training and 20 samples for validation. BraTS consists of 369 multi-modal MRI scans with four modalities (FLAIR, T1, T1Gd, and T2). We divide BraTS into 258, 37, and 74 subjects for training, validation, and testing, respectively.

3.2 Implementation Details

Experimental environment: All experiments are conducted under the same environment (NVIDIA Quadro RTX 6000 GPU; PyTorch 1.11.0). All methods are optimized using the AdamW optimizer [6] with a constant learning rate of $1e-4$ for 500 epochs. **Framework:** We leverage MT [11] as the baseline framework for BvA, in which pseudo labels are generated by the teacher model. V-Net [9] are employed as the segmentation backbone. Dice loss is used as the segmentation criterion \mathcal{L}_{seg} . **Data:** We randomly crop $80 \times 112 \times 112$ (*Depth* \times *Height* \times *Width*) patches for LA and BraTS during training. We set the window size r to half the size of the original slice and the stride $s = 8$ (refer to the hyperparameter experiment in the appendix). **Evaluation metrics:** Dice similarity coefficient (DSC) and average surface distance (ASD) are employed to evaluate segmentation performance in the experiments.

3.3 Comparison with SOTA

We compare BvA with SOTA methods under both barely-supervised and semi-supervised segmentation settings on the LA and BraTS datasets. The compared methods include: SSL (UA-MT [16], CPS [5], and UniMatch [14]), BSL (PLN [7] and DeSCO [4]). The labeled data are set as 5% and 10% of the entire training set respectively, with single-slice annotations for barely-supervised segmentation and complete volumetric annotations for semi-supervised segmentation.

Table 1. Comparison with SOTA methods on the LA dataset with 5% and 10% labeled data. The best results are highlighted in **bold**.

Method	Barely-Supervised Segmentation				Semi-Supervised Segmentation				
	5%		10%		5%		10%		
	DSC (%) ↑	ASD ↓	DSC (%) ↑	ASD ↓	DSC (%) ↑	ASD ↓	DSC (%) ↑	ASD ↓	
SSL	UA-MT [16]	52.51	17.75	56.31	22.28	85.67	2.42	88.41	1.72
	CPS [5]	60.97	7.73	76.95	3.43	88.81	1.83	89.92	1.59
	UniMatch [14]	54.72	5.02	59.19	5.34	88.84	1.82	90.52	1.75
BSL	PLN [7]	66.46	13.34	75.48	7.66	/			
	DeSCO [4]	66.84	14.03	76.21	6.60	/			
	BvA (ours)	87.71	1.62	88.40	1.53	90.80	1.47	91.74	1.37

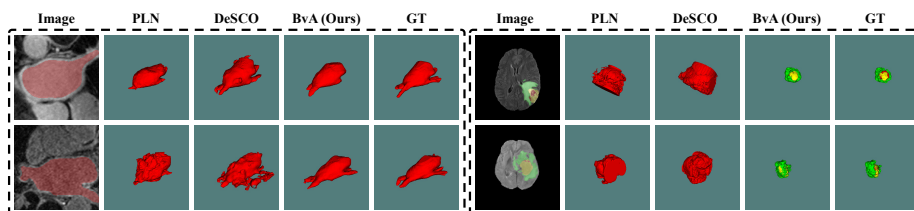
Results on LA As reported in Table 1, BvA sets a new SOTA with 87.71% and 88.40 DSC for barely-supervised segmentation on the LA dataset with 5% and 10% barely-annotated data. For instance, BvA consistently outperforms the registration-based BSS methods, i.e., PLN [7] and DeSCO [4], by a large margin. The inferior performance of the registration-based methods implies that the noisy pseudo labels generated by registration degrade the training process of these models. Besides, the SSL methods yield unsatisfactory results in the BSS setting, which can be attributed to lacking complete volumetric annotations and overfitting on the barely-annotated data. In semi-supervised segmentation, our BvA also achieves the best performance among the compared methods. These results suggest the versatility of BvA for both SSL and BSL scenarios.

Results on BraTS Tumor segmentation is more challenging than organ segmentation due to the heterogeneity of tumors. Table 2 shows the averaged performance of brain tumor segmentation (three-class: enhancing tumor, peritumoral edema, and necrotic tumor core) on the BraTS dataset. On the one hand, BvA achieves 58.42% and 60.47% DSC, and 3.83 and 3.18 ASD, respectively, under 5% and 10% barely-labeled data, presenting considerable improvements compared to the other methods. As image registration cannot capture the heterogeneity of tumors, PLN [7] and DeSCO [4] fail to delineate brain tumors, obtaining unsatisfactory results. Besides, without the impact of registration noise, the SSL methods obtain relatively higher performance than the registration-based approaches. On the other hand, compared to the current semi-supervised SOTA, UniMatch [14], BvA achieves significant gains of 6.36% and 3.80% in terms of DSC. These results further demonstrate the superiority of BvA over the state-of-the-art in both the barely-supervised and semi-supervised settings.

Qualitative Results In Fig. 3, we provide some segmentation examples on the LA and BraTS datasets with 5% barely labeled data. The proposed BvA yields convincing qualitative results for both organ and tumor segmentation, compared with the registration-based methods, i.e. PLN [7] and DeSCO [4]. The reason behind this phenomenon is that the registration noise degrades or even

Table 2. Comparison with SOTA methods on the BraTS dataset with 5% and 10% labeled data. The best results are highlighted in **bold**.

Method	Barely-Supervised Segmentation				Semi-Supervised Segmentation				
	5%		10%		5%		10%		
	DSC (%) ↑	ASD ↓	DSC (%) ↑	ASD ↓	DSC (%) ↑	ASD ↓	DSC (%) ↑	ASD ↓	
SSL	UA-MT [16]	19.81	20.67	23.17	37.31	43.62	2.66	52.89	2.94
	CPS [5]	13.82	50.64	34.07	32.81	65.20	1.81	66.52	2.25
	UniMatch [14]	51.44	9.85	56.06	4.52	60.29	2.34	63.96	1.76
BSL	PLN [7]	5.41	54.09	7.44	57.84	/			
	DeSCO [4]	5.15	57.16	7.40	54.18	/			
	BvA (ours)	58.42	3.83	60.47	3.18	66.64	1.75	67.76	1.79

**Fig. 3.** Qualitative examples on the LA and BraTS datasets. GT: Ground Truth.

overwhelms the training processes of PLN and DeSCO, resulting in qualitatively inferior segmentation. The results are consistent with the performance reported in Table 1 and Table 2, further validating the superiority of BvA for BSS.

3.4 Ablation Study

We conduct an ablation study on the LA dataset with 5% barely-annotated labeled data to investigate the effectiveness of the components of BvA. In Table 3, one can observe that the segmentation performance gradually increases as each component is introduced into our method. Specifically, with NFC to construct a complete volumetric labeled set from the barely-annotated labeled set, the result increases from 71.64% to 76.07% in terms of DSC. Then, FX and SX are adopted to address the style and content domain shifts introduced by NFC, bringing the performance gains of 6.79% and 3.48% in terms of DSC, respectively. Finally, when the domain shifts are alleviated through both the frequency and spatial domain perturbations, BvA improves the segmentation performance to a DSC of 87.71% and an ASD of 1.62. In light of the above, the performance improvement demonstrates that each component contributes positively to the proposed BvA.

4 Conclusion

This paper initially frames barely supervised segmentation as an unsupervised domain adaptation problem, wherein we introduce a novel method, termed BvA.

Table 3. Ablation study of the proposed BvA on the LA dataset under 5% labeled data. F/SX: Frequency/Spatial Mix-Up. The best results are highlighted in **bold**.

Method	Component				5%	
	MT	NFC	FX	SX	DSC (%) \uparrow	ASD \downarrow
Baseline	\checkmark				71.64	9.28
Baseline + NFC	\checkmark	\checkmark			76.07	7.48
Baseline + NFC + FX	\checkmark	\checkmark	\checkmark		82.86	4.39
Baseline + NFC + SX	\checkmark	\checkmark		\checkmark	79.55	5.48
Baseline + NFC + FSX (BvA)	\checkmark	\checkmark	\checkmark	\checkmark	87.71	1.62

Our main ideas lie in the observation that inter-patch similarity in a slice resembles inter-slice continuity in a volume, as well as the assumption that a well-generalized model should exhibit smoothness across domains under small perturbations. The experimental results on the LA and BraTS datasets under both barely-supervised and semi-supervised settings, demonstrate the effectiveness and superiority of BvA over the state-of-the-art.

Acknowledgment

This work was supported by the National Natural Science Foundation of China (Grant No. 62076059).

References

1. Bakas, S., Akbari, H., Sotiras, A., Bilello, M., Rozycki, M., Kirby, J.S., Freymann, J.B., Farahani, K., Davatzikos, C.: Advancing the cancer genome atlas glioma mri collections with expert segmentation labels and radiomic features. *Scientific data* **4**(1), 1–13 (2017)
2. Bakas, S., Reyes, M., Jakab, A., Bauer, S., Rempfler, M., Crimi, A., Shinohara, R.T., Berger, C., Ha, S.M., Rozycki, M., et al.: Identifying the best machine learning algorithms for brain tumor segmentation, progression assessment, and overall survival prediction in the brats challenge. *arXiv preprint arXiv:1811.02629* (2018)
3. Bitarafan, A., Nikdan, M., Baghshah, M.S.: 3d image segmentation with sparse annotation by self-training and internal registration. *IEEE Journal of Biomedical and Health Informatics* **25**(7), 2665–2672 (2020)
4. Cai, H., Li, S., Qi, L., Yu, Q., Shi, Y., Gao, Y.: Orthogonal annotation benefits barely-supervised medical image segmentation. In: *Proceedings of the IEEE/CVF Conference on Computer Vision and Pattern Recognition*. pp. 3302–3311 (2023)
5. Chen, X., Yuan, Y., Zeng, G., Wang, J.: Semi-supervised semantic segmentation with cross pseudo supervision. In: *Proceedings of the IEEE/CVF Conference on Computer Vision and Pattern Recognition*. pp. 2613–2622 (2021)
6. Kingma, D.P., Ba, J.: Adam: A method for stochastic optimization. In: *International Conference on Learning Representations* (2015)

7. Li, S., Cai, H., Qi, L., Yu, Q., Shi, Y., Gao, Y.: Pln: Parasitic-like network for barely supervised medical image segmentation. *IEEE Transactions on Medical Imaging* **42**(3), 582–593 (2022)
8. Menze, B.H., Jakab, A., Bauer, S., Kalpathy-Cramer, J., Farahani, K., Kirby, J., Burren, Y., Porz, N., Slotboom, J., Wiest, R., et al.: The multimodal brain tumor image segmentation benchmark (brats). *IEEE transactions on medical imaging* **34**(10), 1993–2024 (2015)
9. Milletari, F., Navab, N., Ahmadi, S.A.: V-net: Fully convolutional neural networks for volumetric medical image segmentation. In: 2016 fourth international conference on 3D vision (3DV). pp. 565–571. Ieee (2016)
10. Shen, Z., Cao, P., Yang, H., Liu, X., Yang, J., Zaiane, O.R.: Co-training with high-confidence pseudo labels for semi-supervised medical image segmentation. In: Proceedings of the Thirty-Second International Joint Conference on Artificial Intelligence, IJCAI-23. pp. 4199–4207 (2023)
11. Tarvainen, A., Valpola, H.: Mean teachers are better role models: Weight-averaged consistency targets improve semi-supervised deep learning results. *Advances in neural information processing systems* **30** (2017)
12. Xiong, Z., Xia, Q., Hu, Z., Huang, N., Bian, C., Zheng, Y., Vesal, S., Ravikumar, N., Maier, A., Yang, X., et al.: A global benchmark of algorithms for segmenting the left atrium from late gadolinium-enhanced cardiac magnetic resonance imaging. *Medical image analysis* **67**, 101832 (2021)
13. Xu, Q., Zhang, R., Zhang, Y., Wang, Y., Tian, Q.: A fourier-based framework for domain generalization. In: Proceedings of the IEEE/CVF Conference on Computer Vision and Pattern Recognition. pp. 14383–14392 (2021)
14. Yang, L., Qi, L., Feng, L., Zhang, W., Shi, Y.: Revisiting weak-to-strong consistency in semi-supervised semantic segmentation. In: Proceedings of the IEEE/CVF Conference on Computer Vision and Pattern Recognition. pp. 7236–7246 (2023)
15. Yang, Y., Soatto, S.: Fda: Fourier domain adaptation for semantic segmentation. In: Proceedings of the IEEE/CVF conference on computer vision and pattern recognition. pp. 4085–4095 (2020)
16. Yu, L., Wang, S., Li, X., Fu, C.W., Heng, P.A.: Uncertainty-aware self-ensembling model for semi-supervised 3d left atrium segmentation. In: International Conference on Medical Image Computing and Computer-Assisted Intervention. pp. 605–613. Springer (2019)
17. Yun, S., Han, D., Oh, S.J., Chun, S., Choe, J., Yoo, Y.: Cutmix: Regularization strategy to train strong classifiers with localizable features. In: Proceedings of the IEEE/CVF international conference on computer vision. pp. 6023–6032 (2019)
18. Zhang, H., Cisse, M., Dauphin, Y.N., Lopez-Paz, D.: mixup: Beyond empirical risk minimization. In: International Conference on Learning Representations (2018)
19. Zhang, K., Zhuang, X.: Cyclemix: A holistic strategy for medical image segmentation from scribble supervision. In: Proceedings of the IEEE/CVF Conference on Computer Vision and Pattern Recognition. pp. 11656–11665 (2022)
20. Zhang, K., Zhuang, X.: Shapepu: A new pu learning framework regularized by global consistency for scribble supervised cardiac segmentation. In: International Conference on Medical Image Computing and Computer-Assisted Intervention. pp. 162–172. Springer (2022)